Biointerface Research in Applied Chemistry
Open-Access Journal (ISSN: 2069-5837)

Article
Volume 13, Issue 6, 2023, 502
https://doi.org/10.33263/BRIAC136.502

Synthesis and Photophysical Properties of Indolenine Styrylcyanine Dye and its Carboxyl-Labeled Derivative

Svitlana Chernii [1,2,*], Roman Selin [1], Iryna Tretyakova [1], Yan Dovbiy [1], Vasyl Pekhnyo [1], Alexandru Rotaru [3], Viktor Chernii [1], Vladyslava Kovalska [2,†], Andriy Mokhir [4]

1 V.I. Vernadsky Institute of General and Inorganic Chemistry, the NAS of Ukraine, 32/34 Palladin Ave, 03142 Kyiv, Ukraine
2 Institute of Molecular Biology and Genetics, the NAS of Ukraine, 150 Zabolotnogo Street, 03143 Kyiv, Ukraine
3 'Petru Poni' Institute of Macromolecular Chemistry, Romanian Academy, Grigore Ghica Voda Alley 41A, 700487 Iasi, Romania
4 Organic Chemistry II, Friedrich-Alexander-University of Erlangen-Nuremberg, Nikolaus-Fiebiger-Strasse 10, 91058 Erlangen, Germany
† Dr.hab. Vladyslava Kovalska, who initiated, inspired, and supervised this work, suddenly passed away on 03 December 2020.
* Correspondence: chernii.sv@gmail.com;

Scopus Author ID 56024384600
Received: 3.11.2022; Accepted: 5.01.2023; Published: 31.01.2023

Abstract: The indolenine styrylcyanine dye and its carboxyl-labeled derivative were synthesized using condensation of the corresponding indolenines with 4-(dimethylamino) benzaldehyde in the presence of an alkaline catalyst. The spectral-luminescent properties of studied dyes in organic solvents, the aqueous solution (pH 7.9), and the presence of different biomacromolecules were investigated. The functionalization of the dye structure by the carboxylic group led to a bathochromic shift of fluorescence emission spectra while having no impact on dye specificity. It is established that studied styrylcyanines exhibited no or low preference towards biomacromolecules and no accumulation at a specific site within cells.

Keywords: indolenine styrylcyanine dye; fluorescence spectroscopy; absorption; fluorescence microscopy; flow cytometry

1. Introduction

Organic fluorescent dyes are widely used as a working medium in dye lasers [1, 2], in analytical chemistry to determine the various trace elements [2], in photodynamic therapy [3-5], tissue optics [6], and imaging of cells or cell components [6-10]. Depending on the sphere of application of fluorophores, their various properties, including quantum yield [11] and photostability [12], pH dependence [13], or fluorescence lifetime, are essential. Notably, the use of fluorescent dyes for biomedical applications also requires a balance between their photostability and the minimization of the toxicity of their photo-excited products [14, 15]. Even though fluorescent imaging of living cells is a powerful tool in modern biomedical research for detecting and visualizing various biomolecules and cell compartments [16-20], it does not always require fluorescent probes with high quantum yields and other parameters [21].

Among the many existing fluorescent probes, styrylcyanines were earlier reported as promising DNA-sensitive dyes. They demonstrated considerable fluorescence intensity enhancement upon binding to DNA and high fluorescence quantum yield in DNA presence

[22], as well as other biomolecules [23]. In addition, styrylcyanines have a wide range of absorption and emission spectral profiles, which allows for their modification for various applications, including multicolor imaging [24-26]. This unique property of styrylcyanines and the ability of these dyes to be targeted to various cell organelles and their low toxicity [27] opens up many new exciting applications in luminescence imaging. Furthermore, indolenine cyanine dyes have high solubility in solvents and good thermal stability compared with other cyanine dyes. Therefore, such properties of fluorophores could be used as optical information recording and storage materials [28]. Besides, fluorophores not sensitive to biomacromolecules are attractive for labeling prodrugs and pharmaceutics [29-31], which require preserving their active groups during delivery.

Here, we report the synthesis and characterization of two novel indolenine-based styrylcyanine dyes containing a carboxylic group at the indolenine ring, with subsequent testing as potential probes for biological application. The unique design of these dyes makes them suitable candidates for applications in cellular imaging, especially considering the presence of the charged quaternary nitrogen moiety as potential fluorophores for copper(II)-based sensing. Additionally, the presence of a carboxylic group ensures fluorophore bioconjugation since *in vivo* application of fluorophores often requires conjugation to biomolecules, which offers selective localization of fluorophores inside the cells [29]. UV-Visible absorption and fluorescence spectra of these dyes in organic solvents (DMSO, ACN, MeOH), an aqueous solution, and in the presence of biomacromolecules (bovine serum albumin, ovalbumin, *beta*-lactoglobulin, amyloid fibrils of *beta*-lactoglobulin), and nucleic acids (double-stranded DNA, RNA) were investigated. Flow cytometry and fluorescence microscopy studied the ability of dyes to penetrate the living cell membrane and their cell distribution.

2. Materials and Methods

2.1. Materials.

Dimethyl sulfoxide (DMSO), acetonitrile (ACN), methanol (MeOH), 0.05 M Tris-HCl buffer pH 7.9, and HCl solution pH 2 were used as solvents (purchased from Sigma-Aldrich or made from Sigma-Aldrich reagents). Bovine serum albumin (BSA), ovalbumin (OVA), *beta*-lactoglobulin (BLG), as well as high molecular weight double-stranded DNA (dsDNA), and ribonucleic acid of *E.coli* (RNA) were purchased from Sigma-Aldrich (USA). MitoTracker Green, Hoechst 33342 were purchased from ThermoFisher Scientific (Invitrogen).

*2.2. General methods of synthesis of the indolenine styrylcyanine dyes **S1** - (E)-4-(2-(4-(dimethylamino)styryl)-3,3-dimethyl-3H-indol-1-ium-1-yl)butane-1-sulfonate and **S2** - (E)-4-(5-carboxy-2-(4-(dimethylamino)styryl)-3,3-dimethyl-3H-indol-1-ium-1-yl)butane-1-sulfonate.*

4-(Dimethylamino)benzaldehyde (298 mg, 2 mmol) and 590 mg (2 mmol) 4-(2,3,3-trimethyl-3H-indol-1-ium-1-yl)butane-1-sulfonate for **S1**, or 680 mg (2 mmol) 4-(5-carboxy-2,3,3-trimethyl-3H-indol-1-ium-1-yl)butane-1-sulfonate for **S2** were dissolved in isopropyl alcohol (5 ml) by heating and vigorous stirring. Next, piperidine (10 ul) was added to the reaction mixture and refluxed for 3 hours, followed by methyl tert-butyl ether (1 ml). The reaction was cooled down to room temperature, and the formed precipitate was filtered off and washed twice with 2 ml of methyl tert-butyl ether. The crude products were crystallized from 3 ml of isopropanol (dye **S1**) or 3 ml of DMF (dye **S2**). The crystals were filtered off, washed

on the filter with 1 ml of methanol, then twice with 2 ml of methyl tert-butyl ether, and dried at 50°C for 8 hours. The yield was 360 mg (42.2%) for **S1** and 390 mg (41.4%) for **S2**.

*(E)-4-(2-(4-(dimethylamino)styryl)-3,3-dimethyl-3H-indol-1-ium-1-yl)butane-1-sulfonate (**S1**).* Yield 360 mg (42.2%). ^{1}H NMR (300 MHz, DMSO) δ 8.24 (q, *J* = 15.1, 14.9 Hz, 2H), 7.78 (m, 3H), 7.66 (d, *J* = 7.9 Hz, 1H), 7.59 (s, 2H), 7.15 (d, *J* = 8.9 Hz, 2H), 4.92 (m, 2H), 3.54 (s, 6H), 3.45 (m, 2H), 2.57 (m, 2H), 2.47 (m, 2H), 2.07 (s, 6H). ESI MS m/z: Calcd. for $[C_{24}H_{30}N_2O_3S+H]^+$: 427.2050. Found: 427.2035; Calcd. for $[C_{24}H_{30}N_2O_3S+Na]^+$: 449.1869. Found: 449.1835.

*(E)-4-(5-carboxy-2-(4-(dimethylamino)styryl)-3,3-dimethyl-3H-indol-1-ium-1-yl)butane-1-sulfonate (**S2**).* Yield 390 mg (41.4%). ^{1}H NMR (300 MHz, DMSO) δ 8.40 (d, *J* = 15.3 Hz, 1H), 8.28 (s, 1H), 8.17 (d, *J* = 8.4 Hz, 2H), 8.08 (m, 1H), 7.81 (d, *J* = 8.4 Hz, 1H), 7.35 (d, *J* = 15.4 Hz, 1H), 6.90 (d, *J* = 9.0 Hz, 2H), 4.50 (t, *J* = 7.3 Hz, 2H), 3.41 (s, 3H + H_2O), 3.20 (s, 6H), 2.57 (m, 2H), 1.89 (d, *J* = 6.8 Hz, 2H), 1.78 (s, 6H). ESI MS m/z: Calcd. for $[C_{25}H_{30}N_2O_5S+H]^+$: 471.1948. Found: 471.1930; Calcd. for $[C_{25}H_{30}N_2O_5S+Na]^+$: 493.1767. Found: 493.1748.

2.3. Preparation of solutions.

Dye stock solutions were prepared by dissolving the dyes to 2 mM/L concentration in DMSO. Working solutions of free dyes were prepared by diluting the DMSO dye stock solution in 0.05 M Tris–HCl buffer pH 7.9, MeOH, ACN, or DMSO to the final dye concentrations equal to 5 μM/L. The stock solution of proteins (BSA, OVA) was prepared by dissolving the corresponding protein in the Tris–HCl buffer to a concentration equal to 0.2 mg/mL. Working solutions of the dyes in the presence of proteins were prepared by adding the aliquot of the DMSO dye stock solution and the protein stock solutions in the Tris–HCl buffer at a concentration equal to 0.2 mg/mL. The working concentrations of dsDNA and RNA amounted to 6×10^{-5}M bp and 1.2×10^{-4}M bases, respectively. BLG was dissolved at a 5 mg/mL concentration in a water solution of HCl (pH 2). Fibrillar *beta*-lactoglobulin (fBLG) was formed by incubating the protein solution in a Thermomixer incubator at 80°C for 24 hours at pH 2 [32]. All working solutions were freshly prepared before the experiments.

2.4. Spectral measurements.

Spectroscopic measurements were performed in a standard quartz cuvette (10×10 mm). Fluorescence excitation and emission spectra were registered using the fluorescent spectrophotometer Cary Eclipse (Varian, Australia). Absorption spectra were registered using the Shimadzu UV-3600 spectrophotometers. All the spectral-luminescent characteristics of dyes were performed at room temperature.

2.5. Cell cultivation.

The human ovarian cancer cell line (A2780) was purchased from Sigma-Aldrich. A2780 cells were grown in RPMI-1640 medium supplemented with 10% fetal bovine serum (FBS), 1% l-glutamine, and 1% penicillin/streptomycin. Cells were cultivated to 80–90% confluence and detached from the flask using trypsin/EDTA solution (0.025%/0.01%, w/v, Biochrom GmbH, Germany) in DPBS.

2.6. Flow cytometry.

The fluorescence of live cells was quantified using a Guava easyCyteTM 6-2L flow cytometer from Merck Millipore (Darmstadt, Germany) by monitoring the emission at 583±26 nm using a 488 nm excitation light source (yellow fluorescence). For this, detached cells were resuspended in the RPMI-1640 medium containing 5% FBS, 1% L-glutamine, and 1% penicillin/streptomycin and seeded at a concentration of 200 cells/µl per well in a 24-well plate. The plate with a total volume of 0.5 ml per well was left at 37°C in the chamber filled with 5% CO_2 overnight. After 12 hours, the cells were washed (2×0.5 ml DPBS), and a fresh portion of HBSS (0.5 mL) was added. Solutions of dyes **S1** or **S2** in DMSO or DMSO were added into separate wells for 30 min of incubation. The concentration of dyes **S1** and **S2** was 10 or 1 µM/L (1% of DMSO). Then the cells were washed twice with DPBS, and fresh HBSS (0.5 ml) was added. The cells were then trypsin-treated (0.2 ml/w) for 2 minutes and left to dry for 5 minutes in the incubator. Then the fresh HBSS (0.5 ml) was added, and cells were transferred to microtubes. The fluorescence of cells not treated with any dye (containing only the DMSO aliquot as control) and with dyes **S1** and **S2** were quantified. The data were processed using the inCyteTM software package (Merck Millipore).

2.7. Live-cell fluorescence imaging.

For the live-cell staining, detached cells were resuspended in the RPMI-1640 medium containing 5% FBS, 1% L-glutamine, and 1% penicillin/streptomycin and seeded at a concentration of 80 cells/µl per glass-bottom fluorescent dish (µ-Dish 35 mm, high, ibidi GmbH, Germany). Every dish with a 2 ml total volume was left at 37°C in the chamber filled with CO_2 (5%) overnight. After 12 hours, the cells were washed (2×2 ml DPBS), and a fresh portion of HBSS (2 ml) was added. Solutions of Hoechst 33342 and the dyes **S1** and **S2** in DMSO were added into separate and the same dishes for 30 min of incubation. The concentration of dyes was 10 µM/L for **S1** and 20 µM/L for **S2**. Then the cells were washed twice with DPBS, and fresh HBSS (2 ml) was added. The fluorescence images were taken with a Zeiss Axio Vert.A1 and filter set: ex 335–383/em 420–470 nm (blue) to detect Hoechst 33342, ex 450–490/em 500–550 nm (green) to detect MitoTracker Green, ex 538-562/em 570-640 nm (red) for dyes **S1**, **S2**. Objective: 40x/1.30. Oil (DIC). Obtained images were analyzed using the free software Fiji/ImageJ v1.52b [33].

3. Results and Discussion

Indolenine styrylcyanine dyes were synthesized in good yields according to Scheme 1, using 4-(dimethylamino)benzaldehyde and the corresponding indolenine derivative.

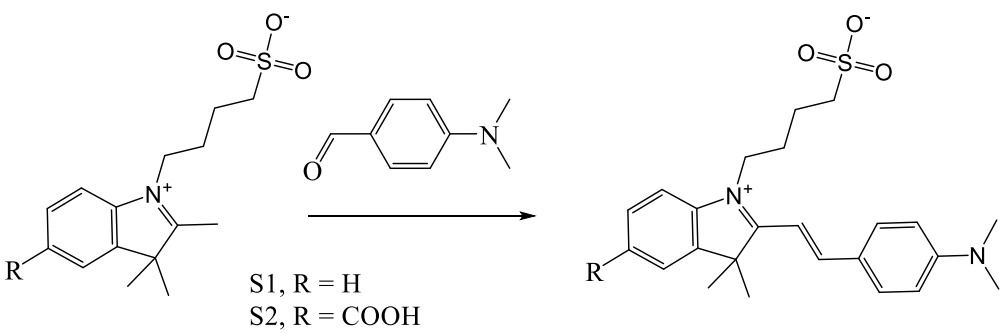

Scheme 1. General synthesis of indolenine styrylcyanine **S1** and **S2**.

The structure of isolated and purified **S1** and **S2** dyes has been confirmed by ^{1}H NMR, ESI-MS spectroscopy, and elemental analysis. The synthesized dyes were subsequently investigated for UV-Vis absorption and fluorescence emission in DMSO, ACN, MeOH, and Tris-HCl buffer (pH 7.9). The UV-Vis absorption spectra data for **S1** and **S2** are summarized in Table 1. In all the investigated cases, the spectra exhibited a broad absorption band between 544-563 nm and, depending on solvent and dye structure, the molar extinction values were moderate in the range (5.3-7.7)×10^4 M^{-1}cm^{-1}. Interestingly, the maximum absorption for both dyes was almost equal in all tested solvents, including the Tris-HCl buffer. The results indicate no apparent interaction between the solvent molecules and the azo dye. In the case of **S2**, introducing a carboxylic group in the indolenine ring led to a bathochromic shift of the absorption maximum concerning the unmodified **S1**.

Table 1. Characteristics of Vis absorption spectra of styrylcyanines in different solvents.

	DMSO		ACN		MeOH		Buffer
	λ_{abs}, nm	ε, 10^4 M^{-1}cm^{-1}	λ_{abs}, nm	ε, 10^4 M^{-1}cm^{-1}	λ_{abs}, nm	ε, 10^4 M^{-1}cm^{-1}	λ_{abs}, nm
S1	550	6.4	544	6.8	549	7.3	548
S2	563	5.3	563	7.7	563	7.0	562

λ_{abs} – maximum wavelength of absorption spectrum; ε – molar extinction coefficient at λ_{abs}.

The emission properties of the **S1** and **S2** dyes in organic solvents were also studied (Table 2). The fluorescence intensity of both compounds in DMSO was 4-5 times higher than in MeOH and ACN. The emission maximum was shifted to the short-wavelength region for both dyes in MeOH (compared to DMSO and ACN). Depending on the solvent, the excitation was located in the 547-564 nm range, with the emission in the 593-609 nm range.

Table 2. Spectral-luminescent properties of styryl dyes in organic solvents.

	DMSO				ACN				MeOH			
	λ_{ex}, nm	λ_{em}, nm	I^{DMSO}, a.u.	*Δ*S, nm	λ_{ex}, nm	λ_{em}, nm	I^{ACN}, a.u.	*Δ*S, nm	λ_{ex}, nm	λ_{em}, nm	I^{MeOH}, a.u.	*Δ*S, nm
S1	553	602	207	49	547	593	45	46	550	593	57	43
S2	564	609	205	45	564	602	35	38	563	599	50	36

λ_{ex} (λ_{em}) – maximum wavelength of fluorescence excitation (emission) spectrum, I - emission intensity of dye in different solvents (I^{DMSO}, I^{ACN}, I^{MeOH}), a.u. – arbitrary units.

Fluorescence spectra in an aqueous solution in the presence of various biomolecules were studied to evaluate the potential of both dyes as probes in fluorescence imaging. The luminescent properties of the studied styrylcyanine dyes in free buffer and the presence of nucleic acids (dsDNA, RNA) are presented in Table 3. The excitation wavelengths of the dyes are located in the range of 550-553 nm for **S1** and 561 nm for S2. The fluorescence emission maxima lie near 592 nm for dye **S1** and 598 nm for dye **S2**, with Stocks shifts between 36-42 nm.

Table 3. Spectral-luminescent properties of styrylcyanines in the presence of nucleic acids.

	Buffer				dsDNA				RNA			
	λ_{ex}, nm	λ_{em}, nm	I_0, a.u.	*Δ*S, nm	λ_{ex}, nm	λ_{em}, nm	I^{DNA}, a.u.	*Δ*S, nm	λ_{ex}, nm	λ_{em}, nm	I^{RNA}, a.u.	*Δ*S, nm
S1	550	592	20	42	551	593	24	42	553	593	23	40
S2	561	599	15	38	561	598	15	37	561	597	16	36

(λ_{ex} (λ_{em}) – maximum wavelength of fluorescence excitation (emission) spectrum, I - emission intensity of dye in a free state (I_0) and in the presence of nucleic acids, a.u. – arbitrary units.).

Both dyes show no significant fluorescence enhancement in the presence of nucleic acids, and no shifts in the excitation and emission spectra were observed upon the addition of nucleic acids.

The luminescent properties of the studied styrylcyanine dyes in the presence of bovine serum albumin (BSA), ovalbumin (OVA), *beta*-lactoglobulin (BLG), and amyloid fibrils of BLG are presented in Table 4. Similarly to the results described above, these dyes displayed little to no fluorescence intensity changes in the presence of tested biomolecules. The excitation wavelengths of the dyes are located in the range of 550-555 nm for **S1** and 562 nm for **S2**. The fluorescence emission maxima are located near 592 nm for dye **S1** and 599 nm for dye **S2**, with Stocks shifts between 36-43 nm. The results show that both dyes do not interact with investigated biomolecules, or the interaction is not assisted in changing the emission properties of the studied styrylcyanine dyes. Furthermore, the carboxylic group does not significantly affect the fluorescence emission intensity of the dyes in the presence of investigated biomolecules.

Table 4. Spectral-luminescent properties of styryl dyes in the presence of different proteins.

	BSA			OVA			BLG			fBLG		
	λ_{ex}, nm	λ_{em}, nm	I^{BSA}, a.u.	λ_{ex}, nm	λ_{em}, nm	I^{OVA}, a.u.	λ_{ex}, nm	λ_{em}, nm	I^{BLG}, a.u.	λ_{ex}, nm	λ_{em}, nm	I^{fBLG}, a.u.
S1	555	593	25	550	592	20	550	592	18	549	592	15
S2	562	598	15	561	599	15	562	599	15	562	599	14

(λ_{ex} (λ_{em}) – maximum wavelength of fluorescence excitation (emission) spectrum, I - emission intensity of dye in the presence of different proteins, a.u. – arbitrary units).

Flow cytometry was used to study the ability of dye **S1** and **S2** to penetrate the cell membrane and specifically accumulate within cellular components.

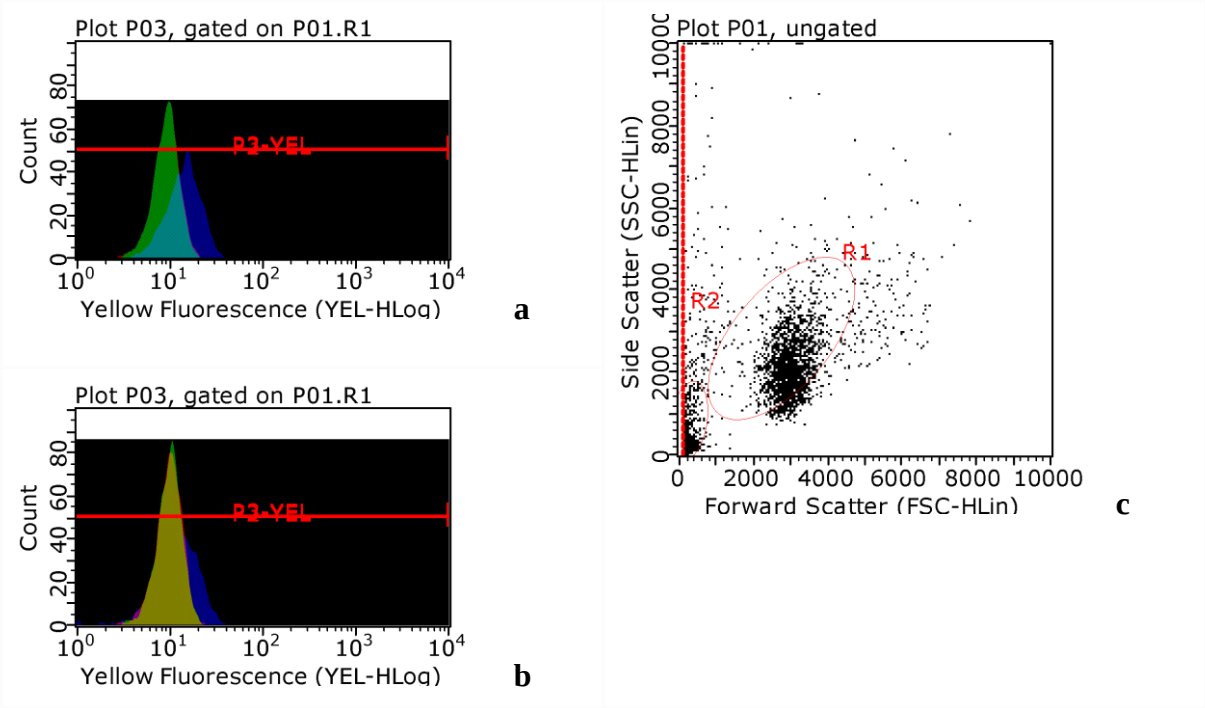

Figure 1. Flow cytometry analysis of the cell membrane permeability of A2780 cell line stained with styryl dyes **S1** and **S2**: (**a)** in concentration 10 µM/L; green profile: cells treated with DMSO; red profile: cells treated with dye **S2**; violet profile: cells treated with dye **S1**; (**b)** in concentration 1 µM/L; green profile: cells treated with DMSO; red profile: cells treated with dye **S2**; violet profile: cells treated with dye **S1**; (**c)** provides information about the internal complexity (i.e., survivability) of the cell.

Both dyes were studied at concentrations of 1 μM/L and 10 μM/L on the human ovarian cancer A2780 cell line. It was observed that the number of cells decreased at elevated concentrations, which may indicate the toxicity of dyes at high concentrations. Figure 1 presents the flow cytometry results for dyes **S1** and **S2** at a concentration of 10μM/L (Figure 1a) or 1μM/L (Figure 1b). For cells treated with dye **S1**, we have observed an increase in the intensity of the yellow fluorescence signal compared to the sample treated with DMSO. Contrarily, the fluorescence intensity of cells in the presence of dye **S2** is almost indistinguishable from DMSO-containing control, which means the fluorescence of the dye is not identified in cells by this method.

Despite the absence of a signal in the flow cytometry experiment for the dye **S2**, it was examined by fluorescence microscopy at similar concentrations. The human ovarian cancer A2780 cell line was used to study the distribution of the **S2** in cells. The working concentration was optimized to 20 μM/L. The fluorescence imaging indicates that **S2** is localized in the cytoplasm (Figure 2a). Commercially available cyanine dyes often efficiently target mitochondria [34].

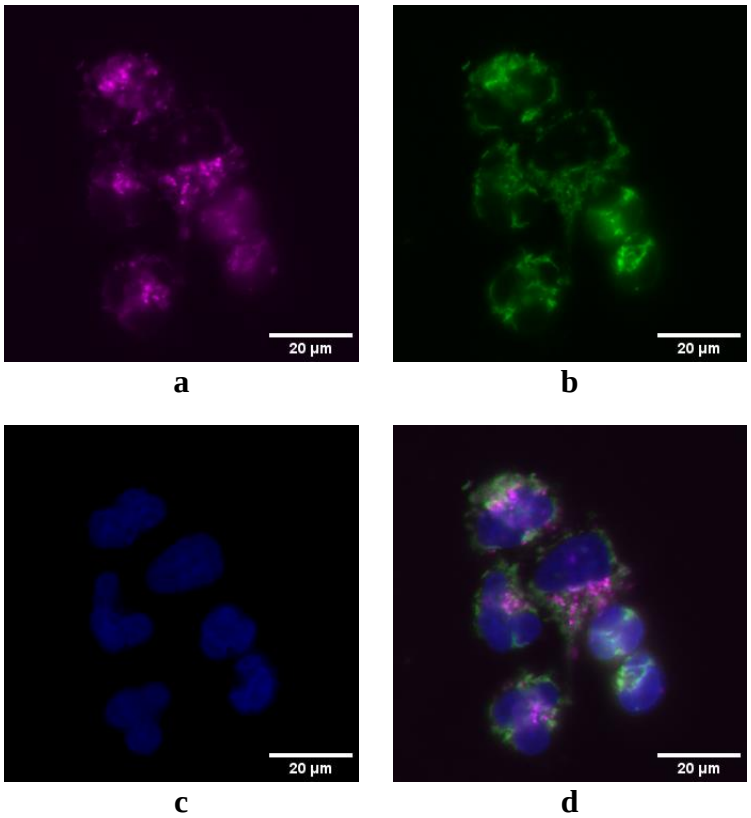

Figure 2. Fluorescence live-cell imaging of A2780 cells: **(a) S2** staining (20 μM/L), **(b)** MitoTracker Green staining (100 nM/L), **(c)** Hoechst staining, **(d)** merged image. Scale bars – 20 μm.

Co-localization of **S2** and mitochondria-targeting standard dye MitoTracker Green (Figure 2b) was carried out to understand the specificity of the dye in cell imaging. In addition, the blue fluorescent standard dye Hoechst binding to nuclear DNA was also used for the co-staining (Figure 2c). This study showed no co-localization of **S2** with MitoTracker Green. Thus, the dye does not penetrate the nucleus nor colocalize with mitochondria in the cytoplasm (Figure 2d). We assume that introducing a negative carboxylic substituent reduces the efficiency of dye penetration into the cell, so the working concentration increases compared to **S1**.

4. Conclusions

In the current investigation, we have presented a synthetic pathway for preparing two novel indolenine styrylcyanine derivatives, with one representative containing carboxylic moiety in its structure suitable for bioconjugation. The new styrylcyanines were characterized by elemental analysis, ^{1}H NMR, ESI-MS, and U.V.–Vis spectroscopy and evaluated for their spectral-luminescent properties in organic solvents (DMSO, ACN, MeOH), an aqueous solution (0.05M Tris-HCl buffer pH 7.9). Additionally, spectroscopic behavior in the presence of a series of biomacromolecules has also been investigated. The absorption maxima of the studied dyes in organic solvents were situated between 544 and 563 nm, with the molar extinction values of (5.3-7.7)×10^{4} $M^{-1}cm^{-1}$ depending on solvent and dye structure. The fluorescence intensity of styrylcyanines in DMSO was 4-5 times higher than in MeOH, ACN, MeOH, or an aqueous solution. The presence of the carboxylic group in the structure of **S2** led to a bathochromic shift of fluorescence emission spectra while having no impact on dye specificity. No changes in the emission and absorption properties of investigated dyes were observed in the presence of tested biomacromolecules; the maximum absorption wavelength and fluorescence emission maximum were identical in the presence and absence of biomacromolecules. Both dyes proved to be cell-permeant, displaying cytoplasmic staining with more or less uniform distribution and no penetration of the nucleus membrane. We assume that introducing a negative carboxylic substituent reduces the efficiency of dye penetration into the cell and, thus, fluorescence imaging. Consequently, **S2** working concentration increases compared to **S1**. Co-localization of **S2** and mitochondria-targeting standard dye MitoTracker Green showed that **S2** does not colocalize with mitochondria in the cytoplasm.

Funding

This research was funded by the European Union's Horizon 2020 research and innovation programme under the Marie Skłodowska-Curie grant agreement number 872331. S.Ch. and R.S. were funded by the scientific research project of young scientists of the NAS of Ukraine No. 0122U002204 for 2022–2023.

Acknowledgments

Our foremost acknowledgment goes to the Armed Forces of Ukraine due to their support that enables us to fulfill this research.

Conflicts of Interest

The authors declare no conflict of interest. The funders had no role in the design of the study; in the collection, analyses, or interpretation of data; in the writing of the manuscript, or in the decision to publish the results.

References

1. Fan, Y.; Zhang, C.; Du, Y.; Qiao, C.; Wang, K.; Hou, Y.; Yao, J.; Zhao, Y.S. A Universal In Situ Cross-Linking Strategy Enables Orthogonal Processing of Full-Color Organic Microlaser Arrays. *Adv Funct Mater* **2021**, *31*, 2103031, https://doi.org/10.1002/adfm.202103031.
2. Kurtaliev, E.N. Spectroscopic study of interaction of styrylcyanine dye Sbt and its derivatives with bovine serum albumin. *J Lumin* **2012**, *132*, 2281–2287, https://doi.org/10.1016/j.jlumin.2012.03.054.

3. Simon, P.; Landl, M.; Breza, M.; Kvasnik, F. New NIR dyes for ammonia sensing. *Sens Actuators B Chem* **2003**, *90*, 9-14, https://doi.org/10.1016/S0925-4005(03)00015-7.
4. Yukruk, F.; Dogan, A.L.; Canpinar, H.; Guc, D.; Akkaya, E.U. Water-Soluble Green Perylenediimide (PDI) Dyes as Potential Sensitizers for Photodynamic Therapy. *Org Lett* **2005**, *7*, 2885–2887, https://doi.org/10.1021/ol050841g.
5. Bassan, E.; Gualandi, A.; Cozzi, P.G.; Ceroni, P. Design of BODIPY dyes as triplet photosensitizers: electronic properties tailored for solar energy conversion, photoredox catalysis and photodynamic therapy. *Chem Sci* **2021**, *12*, 6607-6628, https://doi.org/10.1039/D1SC00732G.
6. Schneckenburger, H.; Wagner, M. Time-Resolved Fluorescence in Biomedical Diagnostics. *In: Geddes, C.D.; Lakowicz, J.R. (eds), Reviews in fluorescence* 2005, 1st ed., Springer Press, Boston, MA, https://doi.org/10.1007/0-387-23690-2_7.
7. Zhang, X.-H.; Wang, L.-Y.; Nan, Z-X.; Tan, S-H.; Zhang, Z-X. Microwave-assisted solvent-free synthesis and spectral properties of some dimethine cyanine dyes as fluorescent dyes for DNA detection. *Dyes Pigm* **2008**, *79*, 205-209, https://doi.org/10.1016/j.dyepig.2008.02.010.
8. Hilal, H.; Taylor, J.A. Determination of the stoichiometry of DNA–dye interaction and application to the study of a bis-cyanine dye–DNA complex. *Dyes Pigm* **2007**, *75*, 483-490, https://doi.org/10.1016/j.dyepig.2006.06.032.
9. Lei, Z.; Zhang, F. Molecular Engineering of NIR-II Fluorophores for Improved Biomedical Detection *Angew Chem Int Ed* **2021**, *60*, 16294-16308, https://doi.org/10.1002/anie.202007040.
10. Liu, Y.; Li, Y.; Koo, S et al. Versatile Types of Inorganic/Organic NIR-IIa/IIb Fluorophores: From Strategic Design toward Molecular Imaging and Theranostics. *Chem Rev* **2022**, *122*, 209–268, https://doi.org/10.1021/acs.chemrev.1c00553.
11. Al-Shamiri, H.A.S.; Abou Kana, M.T.H.; Azzouza, I.M.; Badra, Y.A. Photophysical properties and quantum yield of some laser dyes in new polymer host. *Opt Laser Technol* **2009**, *41*, 415-418, https://doi.org/10.1016/j.optlastec.2008.08.008.
12. Song, B.; Zhang, Q.; Ma, W-H.; Peng, X-J.; Fu, X-M.; Wang, B-S. The synthesis and photostability of novel squarylium indocyanine dyes. *Dyes Pigm* **2009**, *82*, 396-400, https://doi.org/10.1016/j.dyepig.2009.03.002.
13. Mazieres, M.R.; Duprat, C.; Wolf, J.G.; Roshal, A.D. pH-dependent spectral properties and electronic structure of benzothiazol containing cyanine dyes. *Dyes Pigm* **2009**, *80*, 355-360, https://doi.org/10.1016/j.dyepig.2008.08.007.
14. Escobedo, J.O.; Rusin, O.; Lim, S.; Strongin, R.M. NIR dyes for bioimaging applications. *Curr Opin Chem Biol* **2010**, *14*, 64-70, https://doi.org/10.1016/j.cbpa.2009.10.022.
15. Luo, S.; Zhang, E.; Su, Y.; Cheng, T.; Shi, C. A review of NIR dyes in cancer targeting and imaging. *Biomaterials* **2011**, *32*, 7127-38, https://doi.org/10.1016/j.biomaterials.2011.06.024.
16. Aristova, D.; Kosach, V.; Chernii, S.; Slominsky, Y.; Balanda, A.; Filonenko, V.; Yarmoluk, S.; Rotaru, A.; Özkan, H.G.; Mokhir, A.; Kovalska, V. Monomethine cyanine probes for visualization of cellular RNA by fluorescence microscopy. *Methods Appl Fluoresc* **2021**, *9*, 045002, https://doi.org/10.1088/2050-6120/ac10ad.
17. Moshynets, O.; Chernii, S.; Chernii, V.; Losytskyy, M.; Karakhim, S.; Czerwieniec, R.; Pekhnyo, V.; Yarmoluk, S.; Kovalska, V. Fluorescent β-ketoenole AmyGreen dye for visualization of amyloid components of bacterial biofilms. *Methods Appl Fluoresc* **2020**, *8*, 035006, https://doi.org/10.1088/2050-6120/ab90e0.
18. Nag, A.; Das, S. Fluorescent Sensors of Phosphate Containing Biomolecules. *Isr J Chem* **2021**, *61*, 169-184, https://doi.org/10.1002/ijch.202000087.
19. Zhang, Y.; Li, S.; Zhang, H.; Xu, H. Design and Application of Receptor-Targeted Fluorescent Probes Based on Small Molecular Fluorescent Dyes. *Bioconjug Chem* **2021**, *32*, 4–24, https://doi.org/10.1021/acs.bioconjchem.0c00606.
20. Shimomura, T.; Seino, R.; Umezaki, K.; Shimoda, A.; Ezoe, T.; Ishiyama, M.; Akiyoshi, K. New Lipophilic Fluorescent Dyes for Labeling Extracellular Vesicles: Characterization and Monitoring of Cellular Uptake. *Bioconjug Chem* **2021**, *32*, 680-684, https://doi.org/10.1021/acs.bioconjchem.1c00068.
21. Hickey, S.M.; Ung, B.; Bader, C.; Brooks, R.; Lazniewska, J.; Johnson, I.R.D.; Sorvina, A.; Logan, J.; Martini, C.; Moore, C.R.; Karageorgos, L.; Sweetman, M.J.; Brooks, D.A. Fluorescence Microscopy-An Outline of Hardware, Biological Handling, and Fluorophore Considerations. *Cells* **2021**, *11*, 35, https://doi.org/10.3390/cells11010035.

22. Kuperman, M.V.; Snihirova, Y.V.; Kryvorotenko, D.V.; Losytskyy, M.Yu.; Kovalska, V.B.; Yarmoluk, S.M. N-alkylaryl styrylcyanine dyes as fluorescent probes for nucleic acids detection. *Biopolym Cell* **2018**, *34*, 374-386, http://dx.doi.org/10.7124/bc.000987.
23. Chernii, S.V.; Moshynets, O.V.; Aristova, D.I.; Kryvorotenko, D.V.; Losytskyy, M.Yu.; Iungin, O.S.; Yarmoluk, S.M.; Volynets, G.P. Benzoxazole styrylcyanine dye as a fluorescent probe for functional amyloid visualization in Staphylococcus aureus ATCC25923 biofilm. *Biopolym Cell* **2021**, *37*, 447–458, http://dx.doi.org/10.7124/bc.000A6A.
24. Kovalska, V.B.; Kocheshev, I.O.; Kryvorotenko, D.V.; Balanda, A.; Yarmoluk, S.M. Studies on the spectral-luminescent properties of the novel homodimer styryl dyes in complexes with DNA. *J Fluoresc* **2005**, *15*, 215-219, https://doi.org/10.1007/s10895-005-2620-5.
25. Wang, L.; Yang, X.; Chen, X.; Zhou, Y.; Lu, X.; Yan, C.; Xu, Y.; Liu, R.; Qu, J. A novel fluorescence probe based on triphenylamine Schiff base for bioimaging and responding to pH and Fe^{3+}. *Mater Sci Eng C* **2017**, *72*, 551-557, https://doi.org/10.1016/j.msec.2016.11.108.
26. Fan, L.; Fu, Y.J.; Liu, Q.L.; Lu, D.T.; Dong, C.; Shuang, S.M. Novel far-visible and near-infrared pH probes based on styrylcyanine for imaging intracellular pH in live cells. *Chem Commun (Camb)* **2012**, *48*, 11202-4, https://doi.org/10.1039/C2CC35363F.
27. Bohländer, P.R.; Wagenknecht, H.A. Bright and photostable cyanine-styryl chromophores with green and red fluorescence colour for DNA staining. *Methods Appl Fluoresc* **2015**, *3*, 044003, https://doi.org/10.1088/2050-6120/3/4/044003.
28. Chen, P.; Sun, S.; Hu, Y.; Qian, Z.; Zheng, D. Structure and solvent effect on the photostability of indolenine cyanine dyes. *Dyes Pigm* **1999**, *41*, 227–231, https://doi.org/10.1016/S0143-7208(98)00088-6.
29. Ptaszek, M. Rational design of Fluorophores for *in vivo* applications. *In: Progress in Molecular Biology and Translational Science* **2013**, *113*, Academic Press, Elsevier B.V., Netherlands.
30. Sun, D.; Fan, X.; Shi, Y.; Zhang, H.; Huang, Z.; Cheng, B.; Tang, Q.; Li, W.; Zhu, Y.; Bai, J.; Liu, W.; Li, Y.; Wang, X.; Lei, X.; Chen, X. Click-ExM enables expansion microscopy for all biomolecules. *Nat Methods* **2021**, *18*, 107–113, https://doi.org/10.1038/s41592-020-01005-2.
31. Werther, P.; Yserentant, K.; Braun, F.; Grußmayer, K.; Navikas, V.; Yu, M.; Zhang, Z.; Ziegler, M.J.; Mayer, C.; Gralak, A.J.; Busch, M.; Chi, W.; Rominger, F.; Radenovic, A.; Liu, X.; Lemke, E.A.; Buckup, T.; Herten, D.P.; Wombacher, R. Bio-orthogonal Red and Far-Red Fluorogenic Probes for Wash-Free Live-Cell and Super-resolution Microscopy. *ACS Cent Sci* **2021**, *7*, 1561–1571, https://doi.org/10.1021/acscentsci.1c00703.
32. Mazaheri, M.; Moosavi-Movahedi, A.A.; Saboury, A.A.; Khodagholi, F.; Shaerzadeh, F.; Sheibani, N. Curcumin Protects β-Lactoglobulin Fibril Formation and Fibril-Induced Neurotoxicity in PC12Cells. *PLoS One* **2015**, *10*, e0133206, https://doi.org/10.1371/journal.pone.0133206.
33. Schindelin, J.; Arganda-Carreras, I.; Frise, E.; Kaynig, V.; Longair, M.; Pietzsch, T.; Preibisch, S.; Rueden, C.; Saalfeld, S.; Schmid, B.; Tinevez, J.Y.; White, D.J.; Hartenstein, V.; Eliceiri, K.; Tomancak, P.; Cardona, A. Fiji: an open-source platform for biological-image analysis. *Nat Methods* **2012**, *9*, 676–682, https://doi.org/10.1038/nmeth.2019.
34. Lorenz, S.; Tomcin, S.; Mailänder, V. Staining of Mitochondria with Cy5-Labeled Oligonucleotides for Long-Term Microscopy Studies. *Microsc Microanal* **2011**, *17*, 440-445, https://doi.org/10.1017/s1431927611000249.